DETAILED MECHANICS OF MEMBRANE-MEMBRANE ADHESION AND SEPARATION

I. Continuum of Molecular Cross-Bridges

EVAN A. EVANS
Department of Pathology, University of British Columbia, Vancouver, British Columbia, Canada V6T 1W5

ABSTRACT The mechanics of membrane-membrane adhesion are developed for the approximation that the molecular cross-bridging forces are continuously distributed as a normal stress (force per unit area). The significance of the analysis is that the finite range of the cross-bridging forces and the microscopic contact angle are not assumed negligible. Since the cross-bridging and adhesion forces are finite range interactions, there are two membrane regions: a free zone where the membranes are not subject to attractive forces; and an adherent zone where the membranes are held together by attractive stresses. The membrane is treated as an elastic continuum. The approach is to analyze the mechanics for each zone separately and then to require continuity of the solutions at the interface between the zones. Final solution yields the membrane contour and stresses proximal to and within the contact zone as well as the microscopic contact angle at the edge of the contact zone. It is demonstrated that the classical Young equation is consistent with this model. The results show that the microscopic contact angle becomes appreciable when the strength of adhesion is large or the length of the cross-bridge is large; however, the microscopic contact angle approaches zero as the membrane elastic stiffness increases. The solution predicts the width of the contact zone over which molecular bonds are stretched. It is this boundary region where increased biochemical activity is expected. In the classical model presented here, the level of tension necessary to oppose spreading of the contact is equal to the minimal level of tension required to separate the adherent membranes. This behavior is in contrast with that derived for the case of discrete molecular cross-bridges where the possibility of different levels of tension associated with adhesion and separation is introduced. The discrete cross-bridge case is the subject of a companion paper.

INTRODUCTION

Membrane-membrane recognition and subsequent adhesion are prominent processes in biology. In general, these events are dominated by specific molecular binding and cross-bridging reactions. Formation of adhesive contact induces tensions in the membranes that ultimately limit the extent for spreading of the contact. Subsequent separation of an adhesive contact also creates stresses that are transmitted through the membrane to the contact zone. The ideal, classical view is that near equilibrium the forces required to separate membrane-membrane contacts are essentially equal to those induced in the membrane when the adhesive contact is formed. This view, embodied in the well known Young equation (1,2), is based implicitly on the following assumptions: (*a*) the work involved in formation of adhesive cross-bridges is reversible and is thus equal to the work required to separate cross-bridges; (*b*) the cross-bridges are infinitely dense and, consequently, the work to form adhesive contact can be continuously distributed as a free energy reduction per unit area of contact. Also, it is usually assumed that the molecular bridging forces are much shorter range than the scale of membrane curvature changes in the vicinity of the contact zone. (The latter assumption is equivalent to the requirement that the microscopic contact angle, which the membranes form at the first cross-bridge site, is zero.) The result is the Young equation (1,2),

$$\gamma = T_m^o \cdot (1 - \cos \theta_o), \tag{1}$$

where γ is the free energy reduction (chemical affinity) per unit area of contact formation; T_m^o is the membrane tension; and θ_o is the macroscopic contact angle (i.e., the included angle) between the membranes.

In this first paper, the mechanics of membrane-membrane adhesion via continuously distributed cross-bridges are developed for the more realistic situation where the range of the cross-bridging forces is not negligible but is finite in extent. An analytical solution is derived for the case of a continuous adhesive stress that yields the membrane contour and stresses proximal to and within the contact zone as well as the microscopic contact angle at the first cross-bridge site (i.e., at the edge of the contact zone).

It is demonstrated that the classical Young equation is valid. The solution predicts the width of the contact zone over which molecular bonds are stressed. It is this boundary region where increased biochemical activity is expected (e.g., enzyme action, membrane failure, perhaps fusion, etc.).

For the continuum approximation, the level of tension necessary to oppose spreading of the contact is equal to the minimum level of tension required to separate the adherent membranes. In contrast with ideality, experimental observations often show that the tension required to separate a membrane-membrane contact is much greater than the tension induced in formation of the adhesive contact. In fact for some situations, negligible tension is induced by adhesive contact (i.e., there is no spreading) even though the tension necessary to separate the contact is sufficient to rupture the membrane (3)! This appears to be due to a sparse distribution of strong molecular cross-bridges. In a second paper (4), the mechanics of membrane-membrane adhesion and separation is solved for the case of kinetically trapped, discrete cross-bridging forces. The solution is obtained by numerical computation. For the case of discrete molecular cross-bridges, the tension induced by adhesion deviates significantly from the level of tension required to separate the contact as the density of cross-bridges becomes low; the discrete model approaches the continuum approximation as the density of cross-bridges becomes large. Hence, the detailed continuum solution is also necessary as a limiting case for comparison with the solutions for discrete cross-bridging forces.

EXAMPLE OF IDEAL ADHESION/SEPARATION BEHAVIOR

As described in the Introduction, ideal behavior for adhesion and separation of membrane-membrane contacts is identified with mechanical equilibrium and reversibility, i.e., the tensions induced in the membranes as contact is formed are very nearly equal to those required to separate the contact. One situation where ideal behavior has been observed is shown in Fig. 1. Here, two giant phospholipid bilayer vesicles were brought into close proximity and allowed to adhere in the presence of a high molecular weight (36,500 mol wt) glucose polymer (dextran). The vesicle on the right was aspirated with a large suction pressure so that it formed a rigid, spherical test surface because of high tension. The vesicle on the left was allowed to spread on the test vesicle surface to an extent limited by and controlled by its pipette suction pressure. The membrane tension in the adherent vesicle was measured at each equilibrium state as

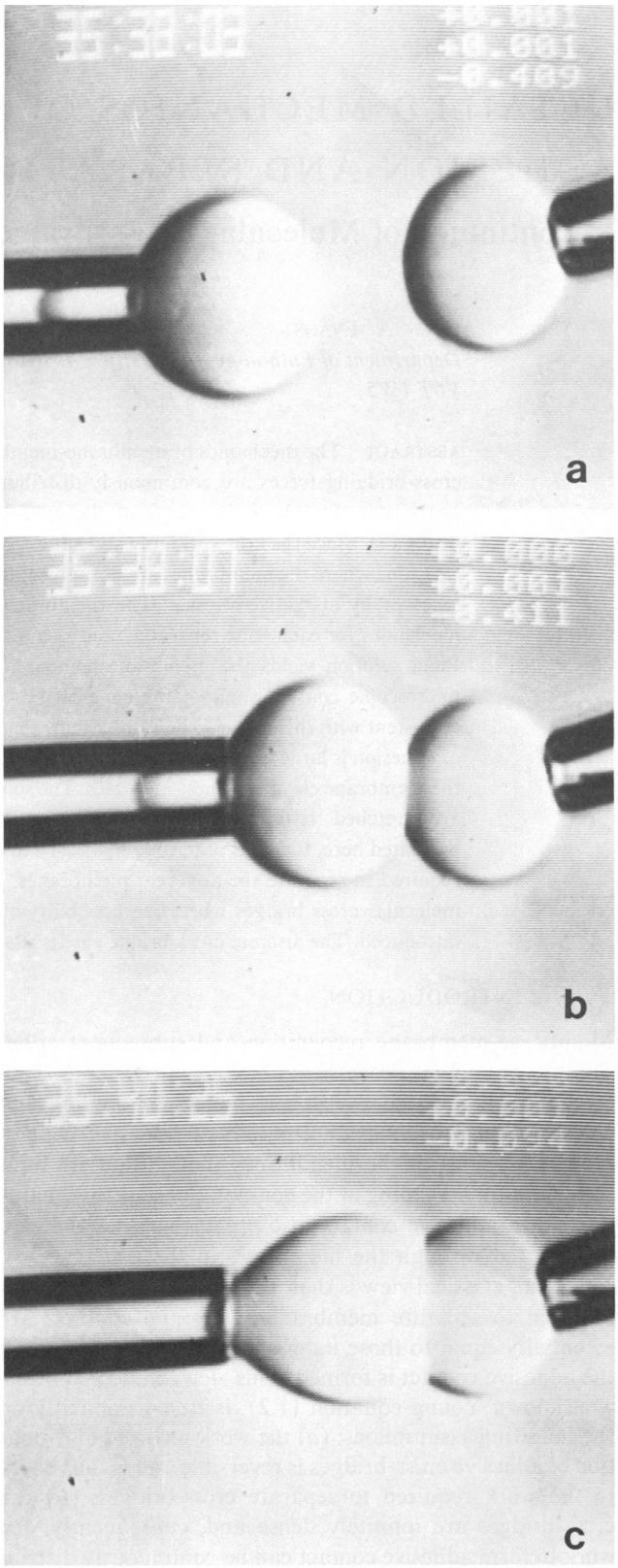

FIGURE 1 Videomicrographs of controlled aggregation of two giant lecithin vesicles in a 10% by weight in grams dextran (36,500 mol wt) and 120 mM salt solution. The vesicles with diameters of 25 and 20 $\times$ 10^{-4} cm were first maneuvered into proximity for adhesion. The vesicle on the right was aspirated with sufficient suction pressure to form a rigid spherical test surface; the vesicle on the left, the adherent vesicle, was held with a low suction pressure that would permit formation of adhesive contact. The left vesicle adhered spontaneously to the rigid vesicle surface and formed a stable equilibrium geometry as shown above. As the pressure was lowered, the left vesicle spread to a new equilibrium configuration with greater contact area (Taken from Evans and Metcalfe, 1984.)

a function of the extent of coverage of the test vesicle surface, both as the contact area was increased and as the contact area was reduced. An example of the results for a single test are shown in Fig. 2 taken from (5). Clearly, the tension levels for contact formation and separation were nearly the same, i.e., there was no hysteresis. Based on a Young type of equation, a single value of the free energy reduction (chemical affinity) per unit area of contact was determined as shown by the correlation curve in Fig. 2. Hence, the lecithin membrane surfaces appeared to adhere via continuously distributed cross-bridges.

An interesting point arises here: binding data for dextrans to cell surfaces (6, 7) indicate that only about 1–10 dextran molecules are bound per 10^4 Å^2 for the range of dextran concentrations used in the vesicle adhesion experiments. This is not sufficient to provide continuous coverage of the surface and yet the adhesion/separation behavior implies otherwise. A possible explanation is found in the results from the second paper (4). These results show that when the scale of the interaction (binding force) between the surfaces is equal to or greater than the distance between cross-bridges, the tension levels for contact formation and separation are comparable. Hence, dextran-mediated adhesion of vesicle surfaces indicates that the range of the dextran interaction between the surfaces is on the order of 100 Å. Since this is much greater than the size of the molecule, the interaction is most likely be due to a gradient in dextran concentration (i.e., a gradient in chemical potential) away from the surface with a scale of 100 Å.

ADHESION MODEL AND MECHANICAL EQUILIBRIUM

The analysis to be presented here considers the cross-bridging and adhesion forces as finite range interactions. Thus, at equilibrium, there are two membrane regions: (*a*) a free (unbridged) zone where the membranes are not subject to attractive forces; and (*b*) an adherent (bridged) zone where the membranes are held together by attractive stresses. This is illustrated in Fig. 3. In the mechanical model, the membrane is treated as an elastic continuum where the attractive stresses are assumed to act normal to the membrane surface. The approach is to analyze the membrane mechanics for each zone separately and then to require continuity of the solutions at the interface between the two zones. In general, membrane curvature proximal to the contact is quite large (i.e., the radius of curvature of the membrane is very small) for an arc normal to the edge of the contact zone; by comparison the curvature of an arc parallel to (or concentric with) the contact zone is very small. Thus, the problem need only be considered in the meridional plane normal to the edge of the contact and depends only on the curvilinear coordinates (s, θ) of the membrane as illustrated in Fig. 3. As such, the membrane supports the intensive forces shown in Fig. 3: a principal tension, T_m, that acts in the plane of the membrane and a transverse shear, Q_m, that acts normal to the membrane (8). The transverse shear is the resultant of bending stresses (moments) in the membrane that are localized to the sharp bend adjacent to and within the adherent zone. In the macroscopic region away from the adherent zone, it is assumed that the membrane is a plane structure under uniform tension, T_m^o; here, the membrane forms a macroscopic (observable) contact angle of θ_o with respect to the other surface.

The local mechanical equilibrium of the membrane in the free, unbridged region is given by the following equations (8): First, the balance of forces tangent to the surface,

$$\frac{dT_m}{ds} - Q_m \cdot K_m = 0. \tag{2}$$

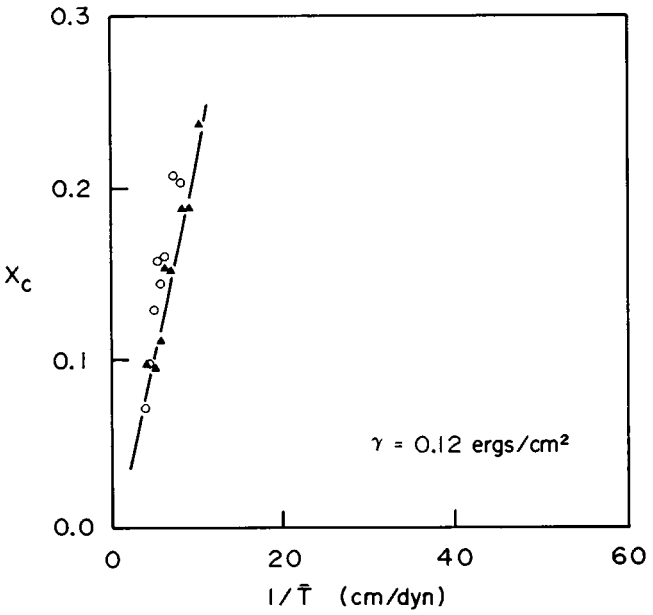

FIGURE 2 Example of data for a single vesicle-vesicle aggregation experiment in a dextran solution. The fractional extent of encapsulation of the rigid vesicle is plotted versus the reciprocal of the tension in the adherent vesicle membrane. The experiment was carried out in 10% by weight in grams dextran (36,500 mol wt) and 120 mM salt solution. The closed triangles represent the formation of adhesive contact whereas the open circles represent subsequent separation of the contact. (Taken from Evans and Metcalfe, 1984).

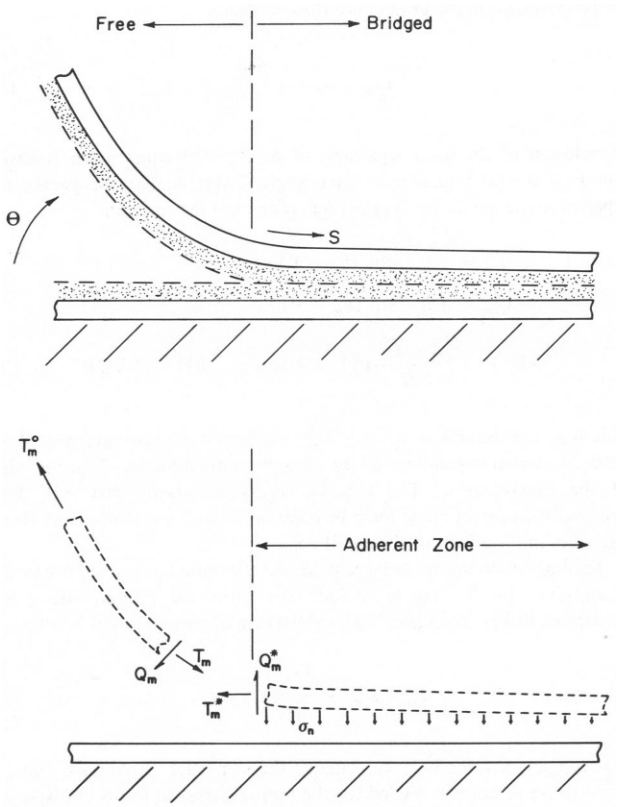

FIGURE 3 Schematic illustration of the adherent (bridged) and free (unbridged) regions adjacent to the edge of the contact zone. The intensive forces supported by the membrane include a principal tension, T_m, that acts tangent to the plane of the membrane surface and a transverse shear, Q_m, that acts normal to the membrane plus the attractive stress, σ_a, which represents the adhesive forces. The curvilinear coordinates (s, θ) are also shown.

Next, the balance of forces normal to the surface,

$$T_m \cdot K_m + \frac{dQ_m}{ds} = 0, \tag{3}$$

where K_m is the local curvature of the meridional arc,

$$K_m = \frac{d\theta}{ds}. \tag{4}$$

To solve these two equations for the unknowns (T_m, Q_m, K_m) the elastic constitutive behavior for the membrane must be introduced, i.e., the elastic relation between force and deformation. In this region of high curvature, the bending or curvature elasticity determines the membrane shape. The elastic constitutive relation for membrane bending is given by the relation that the bending moment (edge couple) is proportional to the change in membrane curvature,

$$M = B \cdot (K_m - K_m^\circ), \tag{5}$$

where K_m° is the stress-free curvature of the membrane and B is the bending or curvature elastic modulus (8). The local balance of moments for the membrane surface yields the relation that the transverse shear is equal to the surface gradient of the bending moment,

$$Q_m = -\frac{dM}{ds}$$

or proportional to the gradient of the curvature,

$$Q_m = -B \cdot \frac{dK_m}{ds}. \tag{6}$$

A solution to the local equations of mechanical equilibrium is easily obtained as a function of curvilinear angle, θ, and the macroscopic tension applied to the membrane in the region far from the contact,

$$T_m = T_m^\circ \cdot \cos(\theta_o - \theta)$$
$$Q_m = T_m^\circ \cdot \sin(\theta_o - \theta)$$
$$(K_m)^2 = \left(\frac{2 \cdot T_m^\circ}{B}\right)[1 - \cos(\theta_o - \theta)] + (K_m^\circ)^2. \tag{7}$$

It is apparent that the transverse shear and membrane curvature increase to maxima that depend on the microscopic contact angle, θ^*, at the edge of the contact zone. The tension, transverse shear, curvature, and microscopic contact angle must be continuous with the solution for these variables in the adherent (bridged) zone.

Turning now to the adherent zone, the equations of mechanical equilibrium in this region include the attractive normal stress, σ_n, illustrated in Fig. 3. Hence, the local balance of normal forces becomes,

$$T_m \cdot K_m + \frac{dQ_m}{ds} = -\sigma_n. \tag{8}$$

The tangential force balance remains the same, Eq. 3. At this point, a constitutive relation is needed for the normal stress in terms of displacement of the membranes from equilibrium (planar) contact. In other words, a model for the molecular adhesion force is required. A reasonable mathematical model for intermolecular force, f_n, is the sum of attractive and repulsive exponential forces as illustrated in Fig. 4. For such a model, there is a maximum force, $\hat{f}_n$, at which the molecular bond will break. The bond length scale, ℓ_b, is the extent of stretch required to reach the peak force. In order to facilitate analysis, the adhesive force is further approximated by a linear force-displacement relation up to the maximum

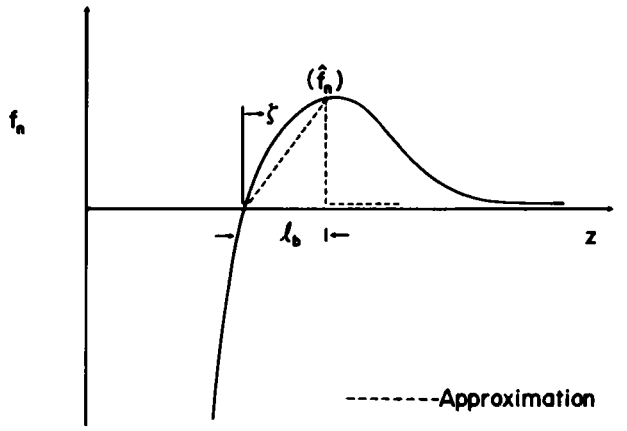

FIGURE 4 Illustration of the model for intermolecular force, f_n, as the sum of attractive and repulsive exponential forces (solid line). The linear force-displacement relation which is used to approximate the intermolecular force is shown as the dashed line. The important characteristics are the bond length, ℓ_b, which is the extent of stretch of the cross-bridge required to reach the breaking point, and the maximum force, $\hat{f}_n$, at which the molecular bond will break.

(breaking) force and zero restoring force for greater bond extensions. The displacement of the bond from equilibrium is represented by the variable ζ; the linearized force relation is thus given by the strength of the bond, $\hat{f}_n$, divided by the bond length, ℓ_b, multiplied by ζ.

$$f_n \cong (\hat{f}_n/\ell_b) \cdot \zeta \quad 0 < \zeta < \ell_b$$
$$f_n \cong 0 \qquad \zeta > \ell_b. \tag{9}$$

In the limit that the cross bridges can be considered as a continuous distribution, the normal stress is modeled by the product of the surface density of receptor sites, $\tilde{n}$, times the force-displacement relation, Eq. 9, $\sigma_n = \tilde{n} \cdot f_n$. For this model, the work necessary to either break or form cross bridges when the membranes are bought together from a large separation distance to planar, equilibrium contact is given by,

$$\gamma \equiv (\tilde{n} \cdot \hat{f}_n \cdot \ell_b)/2, \tag{10}$$

where γ is the adhesion energy or free energy reduction per unit area area of contact formation.[1] In terms of the adhesion energy, the normal stress relation can be rewritten as,

$$\sigma_n = (2\gamma/\ell_b^2) \cdot \zeta. \tag{11}$$

For membrane angles (measured relative to the equilibrium contact plane) that are $\lesssim 30°$, the angle and curvature can be well approximated by the first and second spatial derivatives of the displacement from the equilibrium plane,

$$\theta \cong -\frac{d\zeta}{ds}$$
$$K_m \cong -\frac{d^2\zeta}{ds^2}. \tag{12}$$

With the constitutive relations (Eqs. 6 and 11) plus the geometric

[1]See Appendix A1 for discussion of the relationship between this physical force approach and chemical equilibrium.

relations (Eqs. 12), the local balance of normal forces, Eq. 8, becomes,

$$-T_m \cdot \frac{d^2\zeta}{ds^2} + B \cdot \frac{d^4\zeta}{ds^4} = -(2\gamma/\ell_b^2) \cdot \zeta, \qquad (13)$$

which, in general, must be solved simultaneously with the balance of tangential forces, Eq. 2. The tension term makes Eq. 13 nonlinear but is a higher order (smaller) term in comparison to the bending stress term. Consequently, the variation in tension can be neglected and the tension can be assumed constant just inside the contact zone as a first order approximation; this will allow Eq. 13 to be solved analytically.[2] (Note: with this assumption, the constant value of tension in the contact zone can be approximated by either the initial tension at the edge of the contact zone or the final tension well within the contact zone; the results are little affected by this choice.) With the approximation that the tension is constant, Eq. 13 is solved to give the membrane displacement from equilibrium in the contact zone,

$$\zeta = e^{-\alpha_1 \cdot s} \cdot [C_1 \cdot \sin(\alpha_2 \cdot s) + C_2 \cdot \cos(\alpha_2 \cdot s)], \qquad (14)$$

where the spatial variations are governed by the parameters α_1 and α_2,

$$\alpha_1 = [t + \theta_\alpha^2]^{1/2}/\ell_b$$
$$\alpha_2 = [-t + \theta_\alpha^2]^{1/2}/\ell_b \qquad (15)$$

and,

$$\theta_\alpha \equiv (\gamma \cdot \ell_b^2/2B)^{1/4}$$
$$t \equiv T_m \cdot \ell_b^2/4B. \qquad (16)$$

The displacement is maximum at the edge of the contact zone and decreases exponentially with distance into the contact. The effective width of the boundary layer where molecular bonds are stretched near the edge of the contact zone is given by,

$$\delta \sim \ell_b/\theta_\alpha = (2 \cdot B \cdot \ell_b^2/\gamma)^{1/4}. \qquad (17)$$

It is apparent that the width, δ, will be large when the membrane is stiff (i.e., large bending modulus) and will be small when the adhesion energy is strong (i.e., strong attractive forces between the membranes).

From the contour given by Eq. 14, the displacement, microscopic contact angle, curvature, and transverse shear at the edge of the contact

[2]See Appendix A2 for further discussion of the tension distribution in the contact zone.

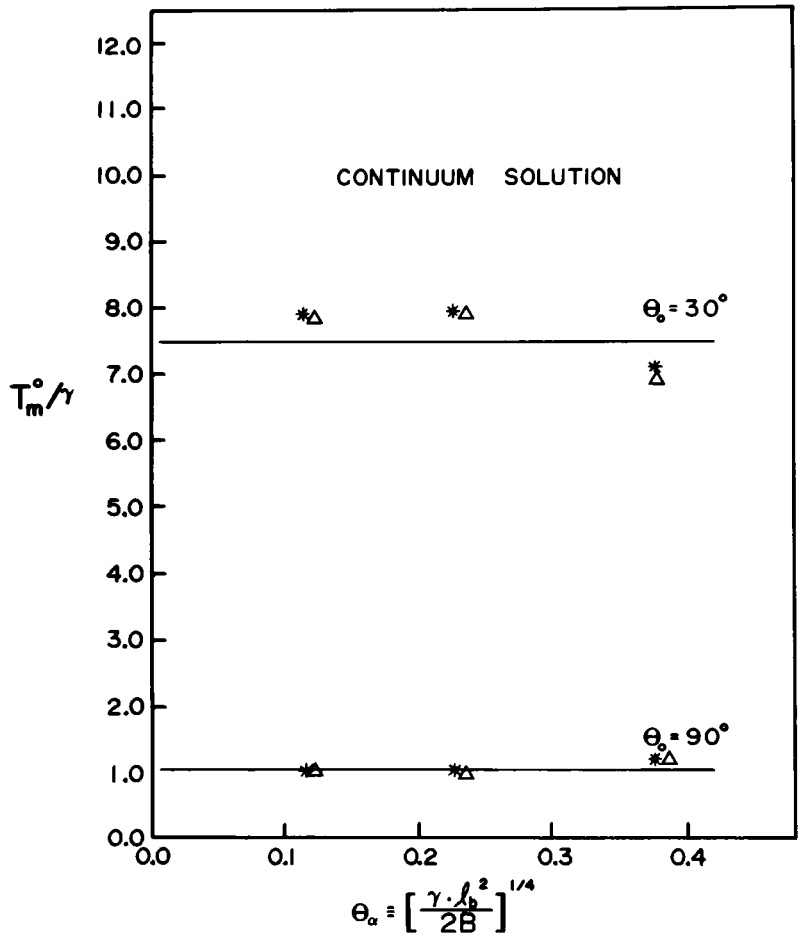

FIGURE 5 The macroscopic tension applied to the membrane in a plane region away from the contact zone, normalized by the adhesion energy per unit area, is plotted vs. the parameter that represents the ratio of adhesion to bending (deformation) energies; two macroscopic contact angles (30° and 90°) were investigated. The results are consistent with the expected values from the Young equation (solid lines). This shows that the classical relation is valid for finite range molecular cross-bridging forces and nonzero microscopic contact angles. Results are shown for two different, constant approximations to the tension within the contact zone; (*) the initial tension at the end of the contact zone; and (Δ) the final tension well within the contact zone.

zone are specified by,

$$\zeta^* = C_2$$

$$\theta^* = \alpha_1 \cdot C_2 - \alpha_2 \cdot C_1$$

$$K_m^* = (\alpha_2^2 - \alpha_1^2) \cdot C_2 + 2\alpha_1 \cdot \alpha_2 \cdot C_1$$

$$Q_m^*/B = [(\alpha_2^2 - \alpha_1^2) \cdot \alpha_1 + 2\alpha_1 \cdot \alpha_2^2] \cdot C_2 + [(\alpha_1^2 - \alpha_2^2) \cdot \alpha_2 + 2\alpha_1^2 \cdot \alpha_2] \cdot C_1, \quad (18)$$

which involve the displacement plus its three spatial derivatives. The displacement at the edge of the contact zone is equal to the maximum bond length, ℓ_b, thus there are only two unknown variables, θ^* and C_1. These are determined by the requirements of continuity with the solution previously derived for the free, unbridged zone, i.e.,

$$\theta^* = \theta$$

$$(K_m^*)^2 = \left(\frac{2 \cdot T_m^\circ}{B}\right)[1 - \cos(\theta_o - \theta^*)] + (K_m^\circ)^2$$

$$Q_m^* = T_m^\circ \cdot \sin(\theta_o - \theta^*).$$

RESULTS AND DISCUSSION

The continuity at the edge of the contact zone of the solutions derived for the free (unbridged) and adherent (bridged) regions can only be satisfied for specific values of the macroscopic tension applied to the membrane, T_m°, and the microscopic contact angle, θ^*. Specific values for these variables are obtained as a function of the dimensionless parameter, θ_α, which represents the ratio of adhesion to bending energies. It is most convenient to consider the macroscopic tension applied to the membrane in the dimensionless form, normalized by the adhesion energy, γ. The ideal, Young equation, Eq. 1, gives a simple relation for this variable in terms of the macroscopic contact angle, θ_o,

$$T_m^\circ/\gamma = (1 - \cos\theta_o)^{-1}.$$

Fig. 5 shows the results for the dimensionless macroscopic tension that result from the continuity requirements at the edge of the contact zone; the results are given for two values of macroscopic contact angle, 30° and 90°. Also, the results are shown for two different, constant approximations to the tension in the contact zone, (*a*) the initial tension at the edge of the contact zone and (*b*) the final tension well within the contact zone. Fig. 5 shows that the classical Young equation is valid for finite-range molecular cross-bridging forces and nonzero microscopic contact angles. The results for the microscopic contact angle as a function of the ratio of adhesion to bending energies is shown in Fig. 6 for the same two values of macroscopic contact angle. It is apparent that the microscopic contact angle is not negligible when the strength of adhesion is large or the bond length is large; however, when the membrane is stiff, the microscopic contact angle approaches zero. For shallow macroscopic contact angles (e.g., 30°), the microscopic contact angle approaches the

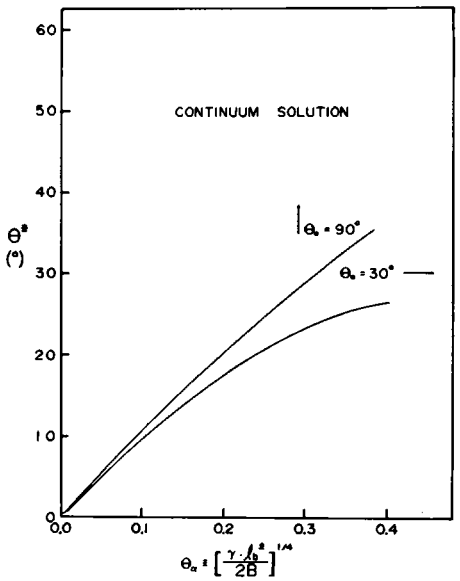

FIGURE 6 The values of the microscopic contact angle are plotted as a function of the ratio of adhesion to bending energies for the same two values of macroscopic contact angle (30° and 90°). The microscopic contact angle becomes appreciable when the strength of adhesion or the bond length is large.

macroscopic value as the ratio of adhesion to bending energies becomes large. As noted previously, the effective width of the boundary layer for which bonds are stretched at the edge of the contact zone is inversely proportional to the ratio of adhesion to bending energies (i.e., Eq. 17). Hence, when the microscopic contact angle becomes large, the width of the boundary layer, δ, is small and there are few bonds stretched at the edge of the contact zone. Fig. 7 shows a membrane contour of the boundary layer region at the edge of the contact zone for a microscopic contact

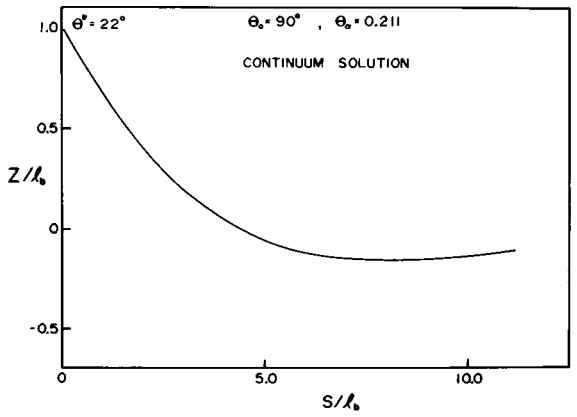

FIGURE 7 A typical membrane contour is plotted vs. the curvilinear coordinate, s, normalized by the bond length, ℓ_b. The specific contour is for a macroscopic contact angle of 90° and a value of 0.211 for the parameter that represents the ratio of adhesion to bending energies. Here, the microscopic contact angle is ~22°. Note that the scale of the displacement axis is greatly expanded.

angle of ~22°. It is interesting to note from this contour that not all of the bonds are stretched; some bonds are slightly in compression.

It is of interest to consider the experimental results obtained for the example discussed of adhesion and separation of giant phospholipid bilayer vesicles in high molecular weight dextran solutions. Here, the free energy reductions per unit area of contact were on the order of 10^{-1} erg/cm^2. The membrane curvature elastic or bending modulus is on the order of 10^{-12} erg (8, 9). With these values, it is possible to estimate the scale of the bond length as a function of microscopic contact angle. For example, if the microscopic contact angle is 10°–20°, then the scale of the bond length would be 40–100 Å. Furthermore, the effective width of the boundary layer over which the bonds are stretched would be on the order of 400–1,000 Å, i.e., ~10 bond lengths.

APPENDIX A1

The purpose of this appendix is to relate the physical force and mechanical energy model, which was used in the text, to the thermodynamics of receptor binding and crossbridge formation. To minimize algebraic complications, it will be assumed that the adhesion is symmetric (i.e., the same size and composition for both membranes). The first important consideration is to determine the time dependent approach to equilibrium. This involves the kinetics of receptor binding and crossbridge formation in relation to the time rate of change of contact area. The critical parameters are three time increments: t_b, the reaction time for binding and cross-bridge formation at fixed local concentrations (that is, without long range diffusional limitations); t_D, the diffusion time for concentration equilibration; and t_m, the mechanical response time for contact area changes. The chemical reaction time, t_b, is essentially determined by local diffusional equilibrium of binding ligands and receptors within the domain occupied by a single receptor. As such, it is most likely limited by the lateral diffusion of receptor sites in the membrane plane, i.e., $t_b \sim \tilde{A}/D = 1/(\tilde{n} \cdot D)$, where $\tilde{A}$ is the surface area per receptor molecule. The chemical reaction time will be negligible in comparison to the diffusion time for concentration equilibration and the mechanical response time for contact area changes. For axisymmetric adhesion, the diffusional time is approximated by the ratio of contact area to surface diffusivity, D, $t_D \sim A_c/D$. The mechanical response time, t_m, is given essentially by the ratio of a surface viscosity to the membrane tension, i.e., $t_m \sim \eta/T_m$ (Evans and Skalak, 1980). Comparison of the diffusional equilibration time to the membrane mechanical response time is represented by the following relation: $t_D/t_m \sim A_c/(t_m \cdot D)$. For cell-size contact areas, the ratio of contact area to lateral diffusivity would range from many seconds to hours for membrane compositions from that of lipid bilayers to red cell membranes respectively (since 10^{-8}cm^2/s $> D > 10^{-13}$cm^2/s). The mechanical response times, t_m, for simple membrane capsules like red blood cells or lipid vesicles are less than a second. Hence for these capsules, membrane adhesive contacts will initially spread without any alteration in receptor densities. For more lethargic mechanical responses such as those exhibited by macrophages and blood granulocytes, the times could become comparable. (For a comprehensive discussion of receptor mobility and binding kinetics in adhesion processes, see Bell, 1978.) It is expected, therefore, that the initial spreading phase of membrane adhesive contacts will be rapid and characterized by local chemical equilibrium of bound and free receptors which will be followed by a much slower time-dependent area change as receptor densities approach global equilibrium by diffusion. At each intermediate state, there will be mechanical equilibrium described by the variational statement that small decreases in free energy due to contact formation plus small increases in work of cellular deformation are balanced to zero,

$$-\gamma \cdot \delta A_c + \frac{\partial W_m}{\partial A_c} \cdot \delta A_c \cong 0.$$

This yields the relationship that the surface affinity equals the derivative of the work of deformation with respect to contact area formation, $\gamma = \partial W_m/\partial A_c$.

Two situations will be considered: (*a*) initial, rapid spreading where the total density of receptors remains uniform and constant; and (*b*) final diffusional equilibrium where the density of free (unbound) receptors is uniform and constant. In both situations, densities and chemical potentials can be treated as constant values within each region (adherent or free) but possibly discontinuous between regions. For constant regional densities, the surface free energy variation is given by the variation of the products of chemical potentials for bound and free receptors times their appropriate populations. When the cross-bridge formation involves two receptors of the same type, the surface free energy variation is expressed as,

$$\delta G = \delta(\mu_b \cdot N_b) + \delta(2\mu_{f_c} \cdot N_{f_c}) + \delta(2\mu_{f_e} \cdot N_{f_e}).$$

On the other hand, if receptors form cross-bridges with other sites on the opposite surface which are in great excess, the surface free energy variation is given by,

$$\delta G = \delta(2\mu_b \cdot N_b) + \delta(2\mu_{f_c} \cdot N_{f_c}) + \delta(2\mu_{f_e} \cdot N_{f_e}).$$

The distinction between these two types of binding reactions will be apparent in the equilibrium constants. The two types will be represented in following development by an asterisk (*) for the appropriate factor of one or two. The N's are the numbers of each component; $\tilde{n}$'s are the local concentrations; and the μ's are the chemical potentials of the components.

Since the local chemical reaction time can be considered much faster than diffusional equilibration and membrane response times, it is assumed that the bound and free receptors in the contact zone are at local chemical equilibrium, i.e.,

$$(*)\mu_b \equiv 2 \cdot \mu_{f_c} + (2 - *)kT,$$

but the unbound (free) receptors in each region are not required to be in equilibrium because of diffusional limitations,

$$\mu_{f_c} \neq \mu_{f_e}.$$

Subscripts (b, f) refer to the bound component and free components respectively; the free components are further differentiated into external (free) and contact (adherent) zones (f_e, f_c). Conservation of receptors dictates,

$$A_c(\delta\tilde{n}_b + \delta\tilde{n}_{fc}) + (A_t - A_c)\delta\tilde{n}_{f_e} = -(\tilde{n}_b + \tilde{n}_{f_c} + \tilde{n}_{f_e}) \cdot \delta A_c.$$

Therefore,

$$\delta G = -[(*)\tilde{n}_b + 2 \cdot \tilde{n}_{f_c} - 2 \cdot \tilde{n}_{f_e}]kT \cdot \delta A_c + (2\mu_{f_e} - 2\mu_{f_c}) \cdot \delta N_{f_e}.$$

The chemical potentials are approximated by

$$\mu_b = \mu_b^\circ + kT \cdot \ell n(\tilde{n}_b/\tilde{n}_o)$$
$$\mu_{f_c} = \mu_f^\circ + kT \cdot \ell n(\tilde{n}_{f_c}/\tilde{n}_o)$$
$$\mu_{f_e} = \mu_f^\circ + kT \cdot \ell n(\tilde{n}_{f_e}/\tilde{n}_o).$$

With the assumption of local chemical equilibrium between bound and free receptors in the contact zone, an equilibrium constant is defined by,

$$K_b \equiv e^{[2\mu_f^\circ - (*)\mu_b^\circ + (2-*)kT]/kT(*)},$$

which is determined by the difference in standard chemical potentials of

the bound and free receptors. Here it is seen that the type of binding reaction establishes the exponent in the equilibrium relation of bound to free receptor concentrations:

$$\tilde{n}_o \cdot \tilde{n}_b/\tilde{n}_{f_c}^2 = e^{[2\mu_f^o - \mu_b^o + kT]/kT}$$

or,

$$\tilde{n}_b/\tilde{n}_{f_c} = e^{[\mu_f^o - \mu_b^o]/kT}.$$

For the initial rapid spreading phase, the total surface density, $\tilde{n}_o$, of receptors is constant, which leads to,

$$\tilde{n}_{f_c} \equiv \tilde{n}_o;\ \tilde{n}_b + \tilde{n}_{f_c} \equiv \tilde{n}_o;\ -\delta N_{f_c} = \tilde{n}_o \cdot \delta A_c,$$

and to the following relation for the surface free energy reduction per unit area of contact formation:

$$-\gamma \cdot \delta A_c = -[(* - 2)\tilde{n}_b]kT \cdot \delta A_c + \tilde{n}_o \cdot kT \cdot \ell n(\tilde{n}_{f_c}/\tilde{n}_o)^2 \cdot \delta A_c.$$

When the binding constant is large, this equation approaches the expected result,

$$-\gamma \cdot \delta A_c \longrightarrow -\tilde{n}_o \cdot [2\mu_f^o - (*)\mu_b^o] \cdot \delta A_c.$$

By comparison, final diffusional equilibrium is characterized by,

$$\mu_{f_c} \equiv \mu_{f_e};\ \tilde{n}_{f_e} \equiv \tilde{n}_{f_c},$$

and the surface free energy reduction per unit area becomes just an excess surface pressure of bound receptors,

$$-\gamma \cdot \delta A_c = -[(*)\tilde{n}_b]kT \cdot \delta A_c.$$

This is the result obtained by Bell and associates (1984) for adhesion of cells without kinetic limitations. The latter depends on the relative contact area ($A_c/A_{total} \equiv \alpha$) since,

$$\tilde{n}_b/\tilde{n}_o = (1 + 2K_b \cdot \alpha - \sqrt{1 + 4K_b \cdot \alpha})/(2K_b \cdot \alpha^2)$$

or

$$\tilde{n}_b/\tilde{n}_o = K_b/(1 + K_b \cdot \alpha).$$

The free energy change per receptor site is given by,

$$\gamma/\tilde{n}_o = [(* - 2)\tilde{n}_b/\tilde{n}_o + \ell n(\tilde{n}_o/\tilde{n}_{f_c})^2] \cdot kT \longrightarrow [2\mu_f^o - (*)\mu_b^o]$$

for the initial spreading phase where receptor concentrations are kinetically restricted (not at diffusional equilibrium). At final diffusional equilibrium, the free energy change per cross-bridge is equal to the thermal energy of each bound complex. It is apparent that the surface affinity, γ, will attenuate with time as the concentration of free (unbound) receptors approaches diffusional equilibrium, i.e.,

$$\ell n(\tilde{n}_{f_e}/\tilde{n}_{f_c})^2 \longrightarrow 0.$$

The free energy reduction per unit area of contact formation, γ, is the free energy change associated with bringing two flat membrane regions from infinite separation to final (force free) equilibrium contact. Displacement, ζ, of the surfaces from the equilibrium contact results in either attractive (increased separation) or repulsive (closer separation) stresses. With the assumptions of linear stress-displacement and finite range interactions, the free energy reduction is a quadratic function of displacement expressed by, γ',

$$\gamma' \simeq \begin{cases} \gamma(1 - \zeta^2/\ell_b^2);\ \zeta < \ell_b \\ 0;\ \zeta > \ell_b \end{cases}$$

where the normal stress is given by,

$$\sigma_n = \frac{\partial \gamma'}{\partial \zeta} \simeq \left(\frac{2 \cdot \gamma}{\ell_b^2}\right) \cdot \zeta$$

From the viewpoint of chemical equilibrium, the displacement of the surfaces from force-free equilibrium produces an increase in the surface free energy that is equivalent to a shift in standard chemical potential for the bound receptors, i.e., a displacement dependent equilibrium constant,

$$K_b' = K_b \cdot e^{(\mu_b^o - \mu_b^\zeta)/kT}$$

where the standard chemical potential, μ_b^ζ, varies from μ_b^o at $\zeta = 0$ to ∞ as $\zeta \rightarrow \ell_b$ the breaking point. It is apparent that in a two-state chemical reaction (bound/free) the concentration of bound receptors decreases with separation if local equilibrium is assumed. This is equivalent to an adiabatic or constant bound receptor density but with an attenuating force per bond.

APPENDIX A2

As discussed in the text, the contribution of membrane tension to the balance of normal forces, Eq. 13, is much smaller than that of the bending stresses. On the other hand, the membrane contour can be used to evaluate the tension distribution in the contact zone. The balance of forces tangent to the membrane is given by the linearized approximation to Eq. 2,

$$\frac{dT_m}{ds} \simeq \sigma_n \cdot \frac{d\zeta}{ds} - B\left(\frac{d^3\zeta}{ds^3}\right) \cdot \left(\frac{d^2\zeta}{ds^2}\right),$$

where the constitutive relation for bending stress has been introduced. Also, it is assumed that the cross-bridge forces act normal to the plane of final contact and, thus, there is a small projection tangent to the membrane surface, i.e., $-\sigma_n \cdot \sin\theta$.

With the contour relation Eq. 14, the tension distribution can be determined. If the small difference between the spatial decay and frequency parameters, α_1 and α_2, is neglected, then $\alpha \equiv \alpha_1 \simeq \alpha_2$ and,

$$\zeta \simeq \ell_b \cdot e^{-\alpha \cdot s}[\tilde{c}_1 \cdot \sin\alpha \cdot s + \cos\alpha \cdot s]$$

$$\frac{dT_m}{ds} \simeq -(2\gamma \cdot \alpha)[(1 + 2\tilde{c}_1 - \tilde{c}_1^2)\sin 2\alpha \cdot s + (1 - 2\tilde{c}_1 - \tilde{c}_1^2)\cos 2\alpha \cdot s] \cdot e^{-2\alpha \cdot s}.$$

For this approximation, integration shows that the tension decreases from T_m-$T_m^o \cdot \cos(\theta_o - \theta^*)$ at the edge of the contact zone to nearly zero at large distances into the contact.

This work was supported by National Institutes of Health grant HL 26965 and Canadian MRC grant MT 7477.

Received for publication 27 June 1984 and in final form 18 January 1985.

REFERENCES

1. Adamson, A. W. 1976. Physical Chemistry of Surfaces. John Wiley & Sons, Inc. New York. 340.
2. Evans, E. A., and V. A. Parsegian. Energetics of membrane deformation and adhesion in cell and vesicle aggregation. *In* Surfaces Phenomena and Hemorheology: Theoretical, Experimental and Clinical Aspects. Copley and Seaman, editors. *Ann. NY Acad. Sci.* 416:13–33.
3. Evans, E. A., and A. Leung. 1984. Adhesivity and rigidity of red

blood cell membrane in relation to WGA binding. *J. Cell Biol.* 98:1201–1208.

4. Evans, E. A. 1985. Detailed mechanics of membrane-membrane adhesion and separation. II. Discrete, kinetically trapped molecular cross-bridges. *Biophys. J.* 48:185–192.
5. Evans, E. A., and M. Metcalfe. 1984. Free energy potential for aggregation of mixed PC:PS lipid vesicles in glucose polymer (dextran) solutions. *Biophys. J.* 457:715–720.
6. Brooks, D. E. 1973. The effect of neutral polymers on the electrokinetic potential of cells and other charged particles. II. A model for the effect of adsorbed polymer on the diffuse double layer. *J. Colloid Interface Sci.* 43:687–699.
7. Chien, S. 1980. Aggregation of red blood cells: an electrochemical and colloid chemical problem. *Adv. Chem. Ser.* 188:1–39.
8. Evans, E. A., and R. Skalak. 1980. Mechanics and Thermodynamics of Biomembranes. CRC Press, Inc., Boca Raton, Florida. 254 pp.
9. Evans, E. A. 1983. Bending elastic modulus of red blood cell membrane derived from buckling instability in micropipet aspiration tests. *Biophys. J.* 43:27–30.
10. Bell, G. I. 1978. Models for the specific adhesion of cells to cells. *Science (Wash. DC).* 200:618–627.
11. Bell, G. I., M. Dembo, and P. Bongrand. 1984. Cell adhesion: competition between nonspecific repulsion and specific bonding. *Biophys. J.* 45:1051–1064.